005

Evaluating Renal Pathology in Post-COVID-19 Human Autopsy Tissues

Elysia A. Masters[1], Mallikarjun Bidarimath[1], Jennifer H. Hanks[2], Vaunita Parihar[3], Amy L. Inselman[1], Jessica J. Hawes[1], Laura K. Schnackenberg[1], Kelly E. Mercer[1]

[1]National Center for Toxicological Research, U.S. Food and Drug Administration, Jefferson, AR 72079

[2]Toxicologic Pathology Associates, Jefferson, AR, 72079

[3]Cancer Tissue and Pathology Shared Resource Core, Winship Cancer Institute of Emory University, Atlanta, GA 30322

Introduction

- Coronavirus disease 2019 (COVID-19), caused by severe acute respiratory syndrome coronavirus-2 (SARS-CoV-2), emerged in late 2019 and continues to circulate globally, infecting over 770 million people with over 6.9 million associated deaths to date (WHO COVID-19 Dashboard).
- Acute kidney injury (AKI) has been reported in as high as 57% of patients hospitalized with COVID-19, with some patients showing long-term signs of kidney injury, such as hematuria and proteinuria [1,2].
- Further, treatment of COVID-19 with the antiviral drug Remdesivir has been associated with increased reporting of kidney disorders [3]. It is currently unknown if the prolonged renal effects following COVID-19 diagnosis are due to systemic infection-related immune responses, direct kidney viral infection, drug toxicity, structural changes of the kidney, or a combination thereof.
- Therefore, the objective of this work was to evaluate kidney tissue samples obtained from autopsies of COVID-19 cases to determine the degree of renal damage and explore possible mechanisms for COVID-19-associated renal nephropathy.

Methods

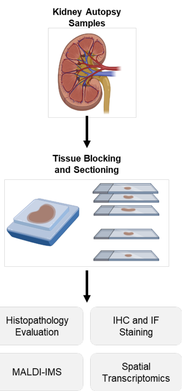

Figure 1. Schematic of experimental design.

Postmortem kidney autopsy samples were collected from reverse transcription polymerase chain reaction (RT-PCR)-confirmed COVID-19 positive cases (N=9) between April and October 2020 (Emory Research University Hospital, Atlanta, GA). Non-infected control kidney autopsy samples were purchased from BioIVT (Westbury, NY). Kidney samples were formalin-fixed and paraffin-embedded before sectioning for downstream analysis. Adjacent sections were used for histopathology evaluation, immunostaining by immunohistochemistry (IHC) and immunofluorescence (IF), spatial glycan analysis by matrix-assisted laser desorption/ionization imaging mass spectrometry (MALDI-IMS) and spatial transcriptomics to evaluation gene expression.

Table 1. Patient Demographics and Metadata

Sample ID	Age	Sex	Race	Cause of Death	Comorbidities	COVID-19 PCR	Symptom Onset to Death (days)	Period of Mech Vent (days)	COVID-19 Medication	SARS-CoV-2 Stain (Lung)
Control 1	67	M	White	Acute myocardial infarction	DM, HTN, Anemia, Myocardial infarction	Negative				Negative
Control 2	67	M	White	Cardiac arrest	CVA, Neuropathy, Pulmonary embolism	Negative				Negative
17	62	M	White, Hispanic	Cardiac arrest	Prior CVA, Seizures, HTN, Hypothyroidism, Depression	Positive	18 d	0	Remdesivir	Positive (ROI)
18	88	F	Black	Cardiac arrest	Dementia, DM, HTN, HLD, Obesity	Positive	Unknown	2 d	None	Negative
22	87	M	Black	Cardiac arrest	Unknown	Positive	Unknown	0	None	Positive (Indv. cells)
23	46	M	Hispanic	Cardiac arrest	None	Positive	37 d	16 d	Tocilizumab, Solumedrol	Negative
37	53	F	Black	Cardiac arrest	Asthma, CHF, CKD, GERD, HTN, Obesity, Seizures	Positive	15 d	7 d	Dexamethasone	Positive (ROI)
38	64	M	Black	Anoxic brain injury, Cardiac arrest	CHF, CKD, HTN, DM, Prior CVA, CAD	Positive	3 d	2 d	None	Positive (ROI)
39						Positive				Negative
40						Positive				Positive (ROI)
44						Positive				Negative

Results

HISTOPATHOLOGY EVALUATION

Table 2. Individual Histopathology Findings

Sample Number	17	18	22	23	37	38	39	40	44	# Abnormal	Mean Score
Infiltrates, interstitial	1	1	1	1	2	1	2	3	0	8	1.3
Glomerulosclerosis	1	2	2	1	1	2	1	3	2	9	1.7
Degeneration, tubular	1	2	0	0	0	0	0	3	0	3	0.7
Mineralization, intratubular	0	1	0	1	1	1	0	0	0	4	0.4
Pigment, intratubular	1	0	2	2	0	1	3	0	0	5	1.0
Intimal thickening, vascular	1	2	0	0	1	0	1	3	2	6	1.1
Thrombosis	0	1	0	0	0	0	0	0	0	1	0.1
Fibrosis, interstitial	1	2	2	1	1	1	1	0	1	8	1.1
Fluid, intratubular	0	2	1	0	0	1	2	0	1	5	0.8
Atherosclerosis	0	1	0	0	0	0	0	0	0	1	0.1
Glomerulopathy, proliferative	0	0	0	0	1	1	0	0	0	2	0.2
Artifact	4	4	4	4	4	4	4	4	4	9	4.0
Sum - Scores:	6	14	8	6	7	8	10	12	6		8.6

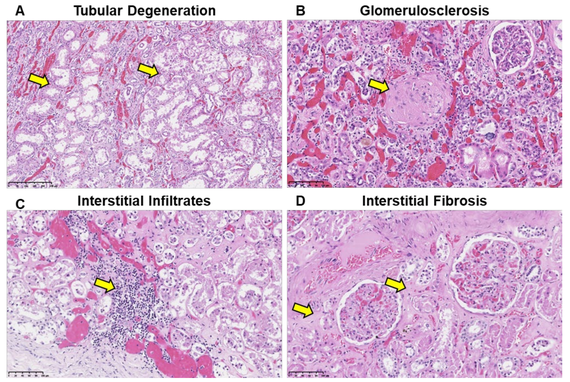

Figure 2. Histopathology examination showed tubular, glomerular, vascular and interstitial changes that were subacute to chronic in nature (Right). Renal autopsy tissues were graded for severity as 1 (minimal), 2 (mild), 3 (moderate) or 4 (marked) to characterize pathologic changes. Notable histological findings were (A) tubular degeneration, (B) glomerulosclerosis, (C) mononuclear to mixed interstitial inflammatory infiltrates (D) interstitial fibrosis and thickening of the vascular intima. Intratubular mineral, fluid, and pigment were noted in multiple samples. Proliferative glomerulopathy, thrombosis, and atherosclerosis were observed in few samples. Due to chronic comorbidities noted by the metadata report, differentiating these findings from acute or subacute SARS-CoV-2 infection is problematic. Additionally, tissue staining was obscured by severe postmortem autolysis.

IMMUNOSTAINING OF IMMUNE CELL INFILTRATES, VIRAL INFECTION AND KIDNEY INJURY MARKERS

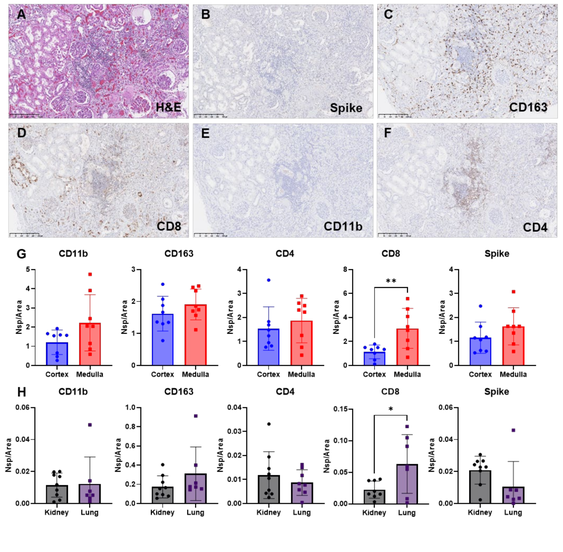

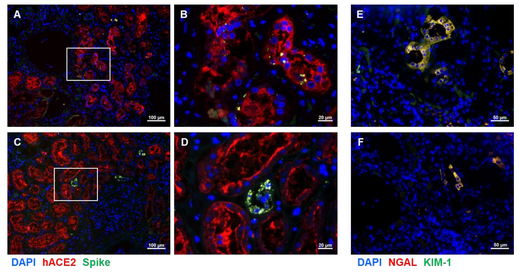

Figure 3. IHC staining of immune cell infiltrates (Left). (A-F) IHC staining of CD11b, CD163, CD4, CD8 and SARS-CoV-2 Spike protein. Staining intensity was quantified by Aperio ImageScope positive pixel algorithm in (G) renal cortex and medullar regions of interest and across (H) patient-matched kidney and lung tissue samples. Due to postmortem autolysis and prolonged exposure of the tissues to formalin fixative prior to embedding some IHC staining appeared faint (CD11b) or non-specific (CD8), thereby limiting any conclusions drawn from these results.

Figure 4. IF staining of viral infection and kidney damage markers (Above). (A-D) hACE2, the receptor for SARS-CoV-2 viral entry into cells, localizes to renal tubules, while Spike protein appears to localize with both regions of abundant hACE2 (top) and regions lacking hACE2 (bottom). (E,F) Markers of acute kidney injury, NGAL and KIM-1, appear to co-stain select renal tubule structures.

SPATIAL DISTRIBUTION OF N-GLYCANS BY MALDI-IMS

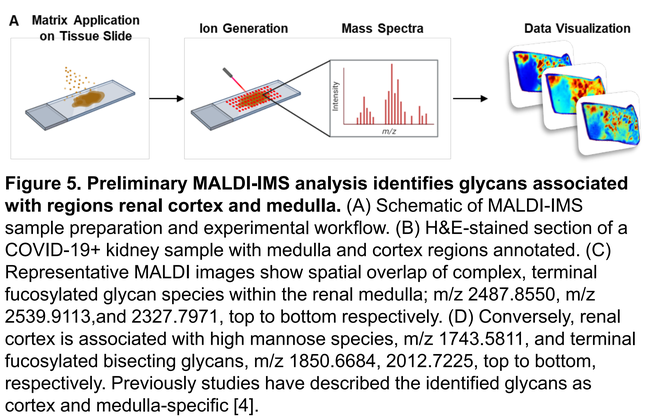

Figure 5. Preliminary MALDI-IMS analysis identifies glycans associated with regions renal cortex and medulla. (A) Schematic of MALDI-IMS sample preparation and experimental workflow. (B) H&E-stained section of a COVID-19+ kidney sample with medulla and cortex regions annotated. (C) Representative MALDI images show spatial overlap of complex, terminal fucosylated glycan species within the renal medulla; m/z 2487.8550, m/z 2539.9113,and 2327.7971, top to bottom respectively. (D) Conversely, renal cortex is associated with high mannose species, m/z 1743.5811, and terminal fucosylated bisecting glycans, m/z 1850.6684, 2012.7225, top to bottom, respectively. Previously studies have described the identified glycans as cortex and medulla-specific [4].

Conclusions

- Taken together, immune cell infiltrate, renal structural changes and possible direct viral infection were all identified in kidney autopsy samples of COVID-19 patients, suggesting a combination of mechanisms that may contribute to COVID-19 associated AKI.
- Consistent with recent literature reports, direct and indirect infection-related kidney injury appeared to be predominately associated within renal tubules [5].
- Due to relatively small sample size, chronic comorbidities of patient samples included and suboptimal tissue processing, the strength of conclusions drawn from this work are limited.

Future Directions

- Additional work currently in progress includes spatial transcriptomic evaluation of COVID-19+ and healthy control tissues to determine differences in gene expression throughout tissue samples (Figure 6).

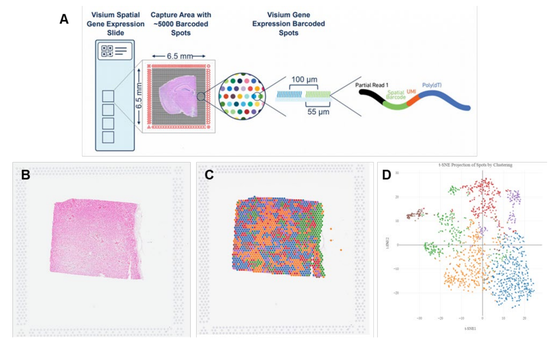

Figure 6. Evaluating spatial gene expression in COVID-19+ kidney tissues. (A) Spatial transcriptomics is a rapidly growing field of study that combines the technology of RNA-sequencing with spatially barcoded information in order to give spatial context to gene expression data. (B-D) Preliminary analysis of kidney autopsy tissues shows tissue spots colored by 10x Genomics automated gene expression clustering algorithm. With these data, we hope to elucidate the mechanism of renal injury during or following COVID-19 disease.

- Ultimately the results of this preliminary study will be used to guide the workflow for follow-up animal and clinical studies to assess long-term renal effects following recovery and treatment for COVID-19.

Acknowledgements

The authors would like to acknowledge the support of TPA Inc for their assistance with this project. This work was supported by FDA/CDER intramural SARS-CoV-2 pandemic fund, FDA COVID-19 supplemental 3 funds, and in part by NIH R33 CA267226 and NIH UO1 CA242096 (R.R.D). Research reported in this publication was supported in part by the Cancer Tissue and Pathology shared resource of Winship Cancer Institute of Emory University and NIH/NCI under award number P30CA138292.

Disclaimer: This poster reflects the views of the authors and does not necessarily reflect those of the U.S. Food and Drug Administration. Any mention of commercial products is for clarification only and is not intended as approval, endorsement, or recommendation.

References: [1] Hirsch, J., et al., Kidney Int, 2020. [2] Glowacka, M., et al., Int J Mol Sci, 2021. [3] Humeniuk, R., et al., Clin Transl Sci., 2020. [4] Drake, R., et al., Mass Spec, 2020. [5] Diao, B., et al., Nature Comm., 2021.